(2)

ARMY RESEARCH LABORATORY

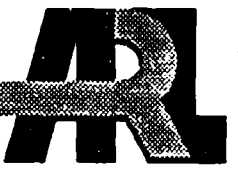

Mechanical Response of Gun Propellant Beds at Low Strain Rates

Robert J. Lieb
Michael G. Leadore

ARL-TR-78 February 1993

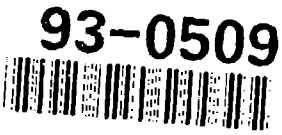

NOTICES

Destroy this report when it is no longer needed. DO NOT return it to the originator.

Additional copies of this report may be obtained from the National Technical Information Service, U.S. Department of Commerce, 5285 Port Royal Road, Springfield, VA 22161.

The findings of this report are not to be construed as an official Department of the Army position, unless so designated by other authorized documents.

The use of trade names or manufacturers' names in this report does not constitute indorsement of any commercial product.

REPORT DOCUMENTATION PAGE

Form Approved
OMB No. 0704-0188

1. AGENCY USE ONLY *(Leave blank)*	2. REPORT DATE	3. REPORT TYPE AND DATES COVERED
	February 1993	Final, June 92 - Aug 92

4. TITLE AND SUBTITLE

Mechanical Response of Gun Propellant Beds at Low Strain Rates

5. FUNDING NUMBERS

1L161102AH43

6. AUTHOR(S)

Robert J. Lieb and Michael G. Leadore

7. PERFORMING ORGANIZATION NAME(S) AND ADDRESS(ES)

8. PERFORMING ORGANIZATION REPORT NUMBER

9. SPONSORING/MONITORING AGENCY NAMES(S) AND ADDRESS(ES)

US Army Research Laboratory
ATTN: AMSRL-OP-CI-B (Tech Lib)
Aberdeen Proving Ground, MD 21005-5066

10. SPONSORING/MONITORING AGENCY REPORT NUMBER

ARL-TR-78

11. SUPPLEMENTARY NOTES

12a. DISTRIBUTION/AVAILABILITY STATEMENT

Approved for Public Release - Distribution is Unlimited

12b. DISTRIBUTION CODE

13. ABSTRACT *(Maximum 200 words)*

A device was designed and built to measure the applied transmitted and central stresses within propellant beds of JA2, M30, and M43 gun propellants during compaction. It was observed that the stress at the center of the beds matched the average applied stress in form and magnitude in all but one instance. The velocities of mechanical disturbances were calculated and found to range from 50 to over 300 m/s. A strong correlation was demonstrated between the single grain and bed modulus values.

14. SUBJECT TERMS

Mechanical Response, Propellants, Bed, M30, JA2, M43, Stress Profile, Strain Rate

15. NUMBER OF PAGES

24

16. PRICE CODE

17. SECURITY CLASSIFICATION OF REPORT	18. SECURITY CLASSIFICATION OF THIS PAGE	19. SECURITY CLASSIFICATION OF ABSTRACT	20. LIMITATION OF ABSTRACT
UNCLASSIFIED	UNCLASSIFIED	UNCLASSIFIED	SAR

Intentionally Left Blank

TABLE OF CONTENTS

Intentionally Left Blank

LIST OF FIGURES

LIST OF TABLES

Intentionally Left Blank

1. INTRODUCTION

The response of gun propellant to mechanical stress plays a critical role in the evolution of pressure during the ballistic cycle. Stress communicated through the bed can produce projectile motion[1], which can critically affect the early ignition conditions. If stress levels exceed critical values grain fracture can result which produces unprogrammed surface area and results in an accelerated pressurization. The sound speed (the propagation of a mechanical disturbance) within the granular bed is also determined by the bed response[2,3]. Factors, such as the propellant impetus, flame spreading, grain geometry, propellant burning rate, the ignition system, and many others interplay to influence the pressurization rate during combustion. The more that is known about the nature of the bed response, the more that will be understood about the interplay among the parameters.

Most of the testing done to determine the mechanical response of granular beds has been done at low rates on conventional testers[4,5,6,13]. Some explosive loading techniques have been employed to increase the rate of testing and to simulate the loading profile believed to be experienced by the bed during ignition[7]. In all of these tests the problem of the bed interaction with the wall of the chamber has always been difficult to address. In an earlier paper[8] a special measurement arrangement was designed to isolate the wall from influencing the force measurement on the bed. These tests were conducted at higher rates (about 50/s) to more closely approach operational conditions, but the measurements were limited to very low strains and impulsive loading profiles because of the drop weight arrangement used to deliver the load. Results from those tests, however, seemed to indicate that stress measurements were isolated from wall effects.

In the current study, investigations into the nature of the stress profile across the bed were conducted. This required higher strains and more controlled strain rates than could be attained using drop-weight loading, and necessitated the use of a device that could deliver a significantly higher load. A conventional tester was used with a testing apparatus based on the design of the tester used in Reference 8, but modified to include a measurement of the transmitted stress. This arrangement permitted the investigation of the axial and radial stress profile across the bed.

2. EXPERIMENTAL PROCEDURE AND RESULTS

2.1 Description of the Tester. The bed tester is illustrated in Figure 1. It consists of a ram, cylinder, and anvil which was used to compress the bed of granular propellant. The gage at the top of the ram measured the force applied to the bed. The ram guide rested on the bed wall, kept the ram shaft in the center of the bed, and helped to keep the applied strain uniform. The bed itself had a

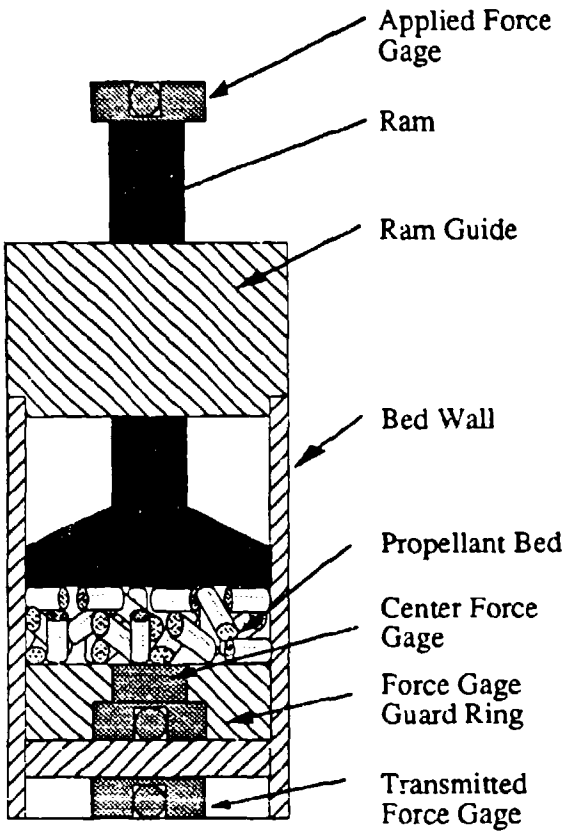

Figure 1. Schematic Diagram of the Bed Tester

Table 1. Propellant Grain Dimensions

Type	Length (mm)	Dia. (mm)	Perforation Dia. (mm)	Perforation Number
JA2	14.91	9.89	0.84	7
M30	17.60	7.15	0.69	7
M43	13.75	8.28	0.33	19

nominal length of 4 cm and a diameter of 8.29 cm (surface area of 53.9 cm^2). The dimensions of the tested grains are found in Table 1. The bottom of the bed was supported by a second force gage at the center of the bed and by an annular steel guard ring which had its top surface flush with the top of the gage. The second gage permitted measurement of the stress at the center of the bed over an area of 5.07 cm^2, about 10 percent of the total bed area, while the ring supported the balance of the bed area. The second gage and the ring rested on a steel plate that was supported by a third force gage. This gage was supported by the cross-head, as was the bed wall. This arrangement permitted measurement of the stress transmitted through the bed, and, thereby, provided a measure of the axial bed stress transmitted to the wall through shear. The temperature conditioned bed assembly was removed from the conditioning chamber and placed on the cross-head of an Model TT-C Instron Tester and compressed by raising the crosshead. The displacement of the crosshead was measured using a Linear Variable Differential Transformer.

The four channels of data (displacement, applied force, transmitted center force, and total transmitted force) were recorded at 5-ms intervals at a strain rate of about 0.02 s^{-1}. Stress values were calculated by dividing the measured forces by the corresponding areas.

Compliance measurements were performed and the tester-machine assembly was found to have a linear stiffness of 45.7 kN/mm. The strain was calculated by correcting the displacement readings for this compliance and dividing the corrected displacement by the initial bed height.

Table 2. Nominal Percent Composition and Densities of Propellants

	JA2	M30	M43
Composition			
Nitrocellulose (NC)	59	28	4
NC Nitration Level	13.1	12.6	12.6
Nitroglycerin (NG)	15	22	
Nitroguanidine (NQ)		48	
Ethyl Centralite (EC)		2	
Diethylene Glycol Dinitrate	25		
Akardit II	1		
RDX (Ground)			76.0
Cellulose Acetate Butyrate			12.0
Plasticizer			8
Densities			
ρ_s (g/cm^3)	1.58	1.66	1.66
ρ_l (g/cm^3)	0.920	0.900	0.953

Tests were performed at bed temperatures of -32°C, 23°C, and 52°C using JA2, M30, and M43 propellants, whose formulations are listed in Table 2. The period of temperature conditioning was selected based on cooling and heating experiments performed on propellant beds. It was found that the center of the propellant bed reached the conditioning temperature in 120 minutes, when the assembly shown in Figure 1 was placed in the conditioning chamber which was set to the desired temperature. After conditioning, it was also found that the bed remains at the desired temperature for 4.0 minutes before the ambient conditions begin to change the temperature around the bed. Where ever possible three repetitions were performed for each test condition. The bed height of 4 cm (nominal) was chosen based on the results of bed testing performed in Reference 8. In those tests it was determined that beds of at least this height were required for grains of this size before the scatter in the measurements was reduced to an acceptable level.

2.2 Test Results. Figure 2 shows the average results of the JA2 propellant bed tests. The applied, center, and transmitted stress are presented as a function of strain at each of the three temperatures. Figures 3 and 4 show the same information for M30 and M43, respectively. In every case, the applied stress is somewhat larger than the transmitted stress, as expected, since the force transmitted to the wall by the bed is not measured by the transmitted force gage. The stress at the center of the bed follows the same trends as the applied and transmitted stresses, but the magnitude of the stress has some variability from propellant to propellant. For JA2 the center stress was significantly below the

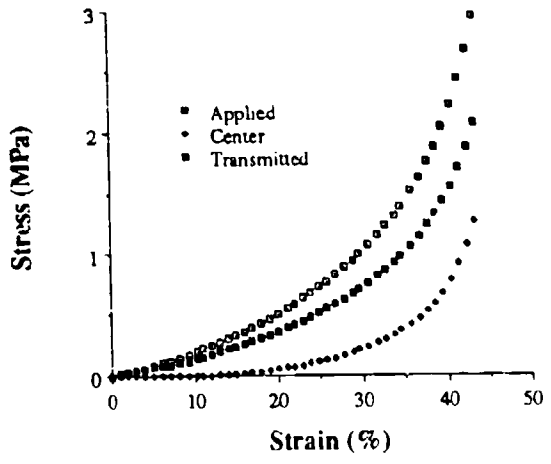

a. JA2 at 52°C

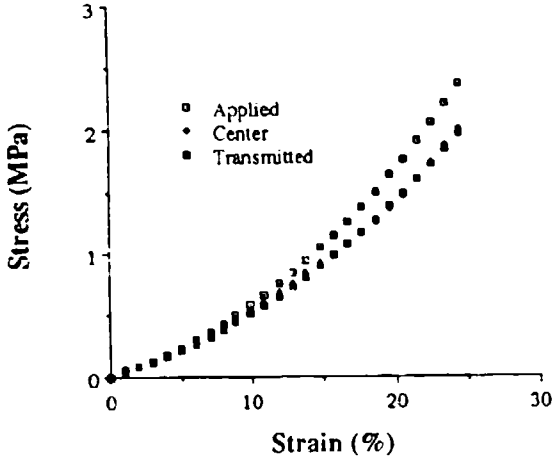

b. JA2 at 23°C

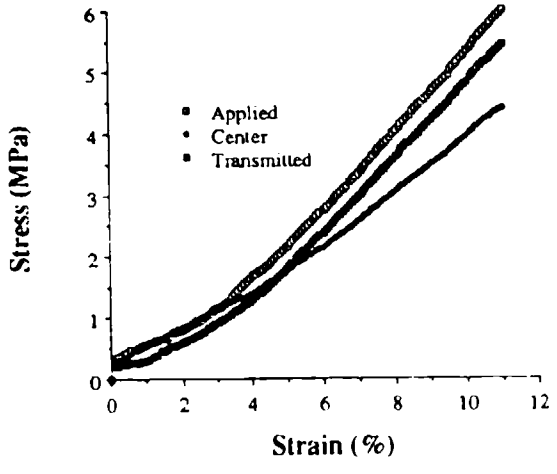

c. JA2 at -32°C

Figure 2. Bed Responseof JA2

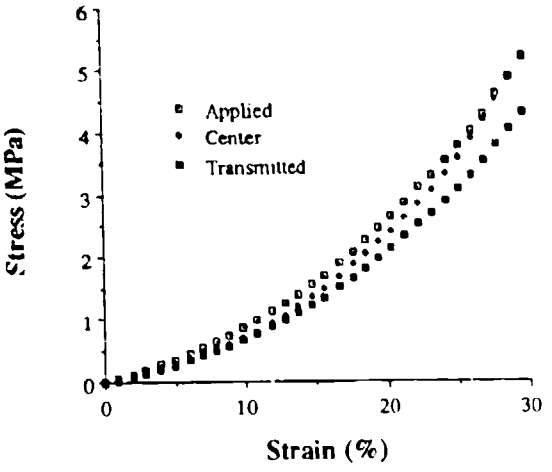

a. M30 at 52°C

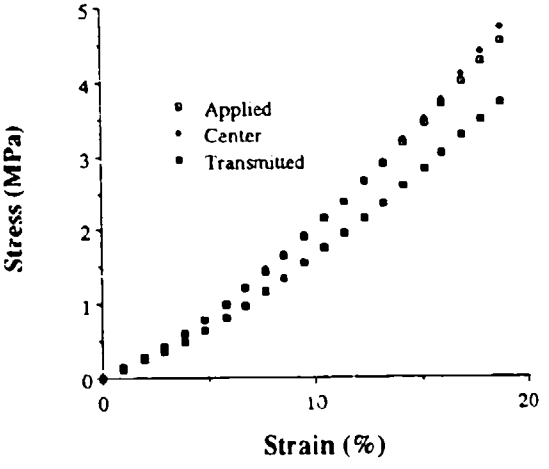

b. M30 at 23°C

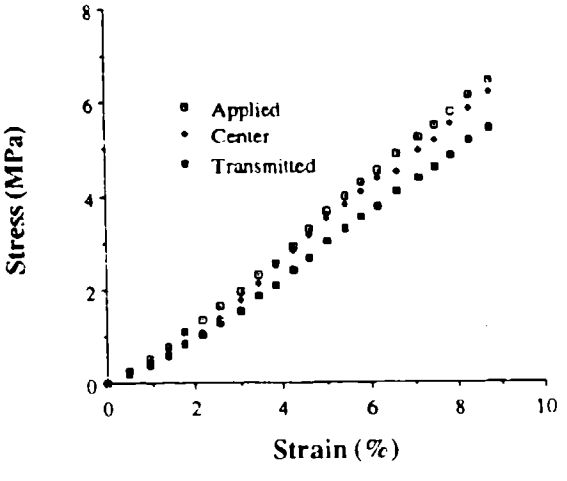

c. M30 at -32°C

Figure 3. Bed Responseof M30

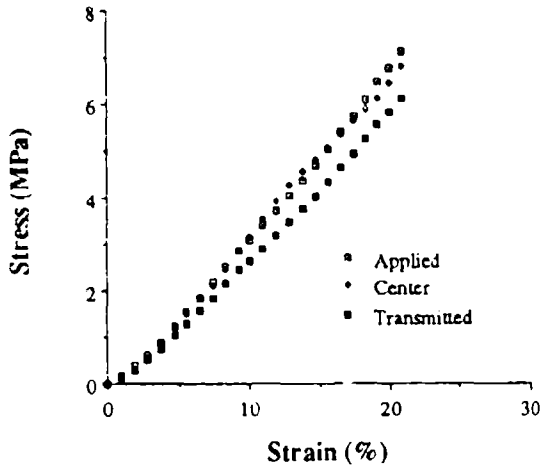

a. M43 at 52°C

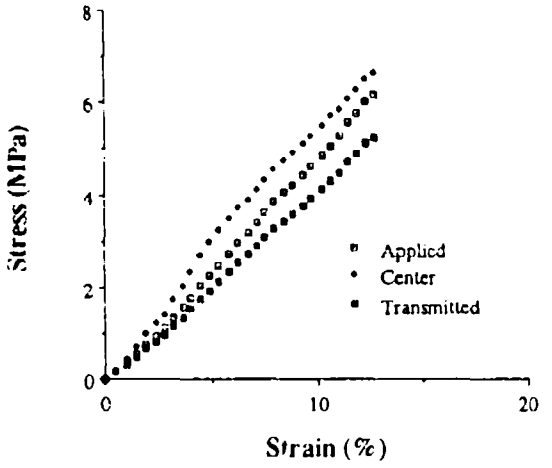

b. M43 at 23°C

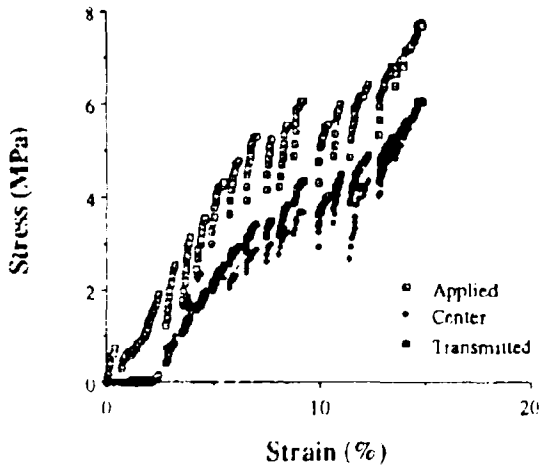

c. M43 at -32°C

Figure 4. Bed Responseof M43

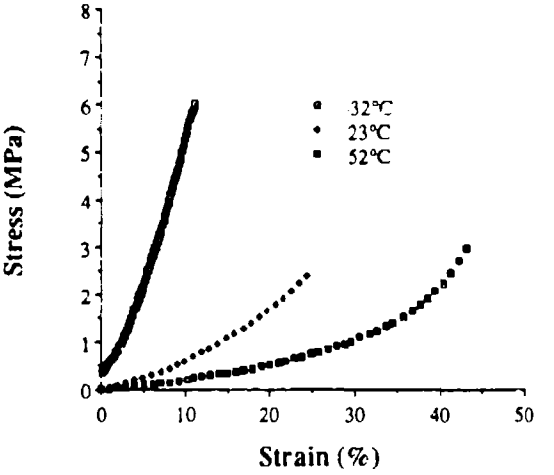

a. JA2

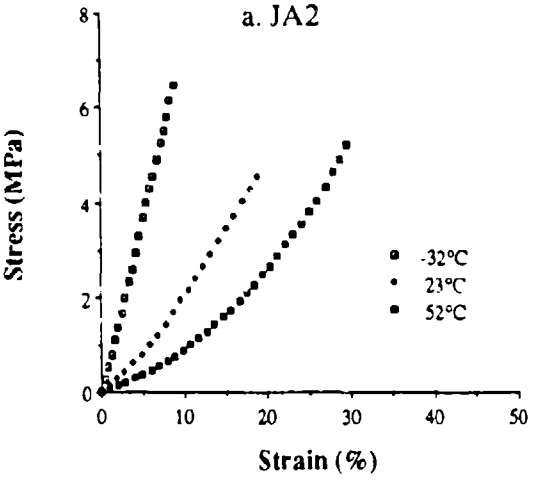

b. M30

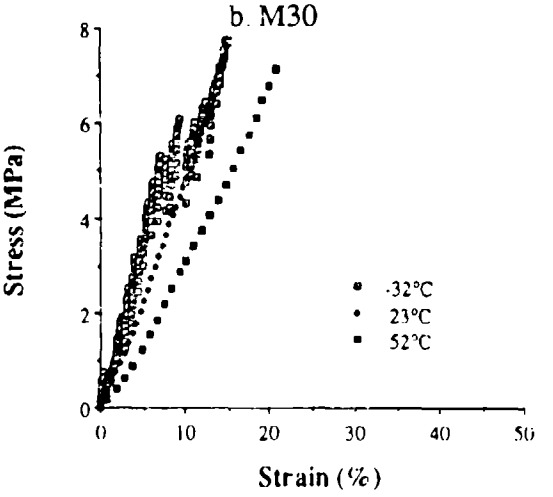

c. M43

Figure 5. Applied Stress vs Strain

other two stresses at the high temperature and matched the transmitted stress at 23°C. For M30 the center stress closely followed the applied stress in all cases, and for M43 the center stress again matched the applied stress for high and ambient temperatures, with the center exceeding the applied at 23°C. At -32°C sever fracture was recorded for M43 and the center stress followed the transmitted stress closely in both magnitude and form. Figure 5 compares the applied stress at each temperature for each of the propellants to show the effect of temperature on the bed response.

3. ANALYSIS

In all but a few cases the response of the propellant beds was measured until maximum loads were experienced on the test frame. JA2, which is significantly softer than the other propellants, was tested first and was not taken to maximum load until the low temperature response was measured. This is the reason that the levels of stress are lower for JA2. Of particular interest in this study is the change in bed response with increasing strain and decreasing porosity. This response determines the stiffness of the bed (the bed modulus) and the sound speed (the propagation of a mechanical disturbance) within the bed. The onset and the degree of fracture damage that the bed suffers also affect the interior ballistic cycle. Each of these considerations is addressed for each propellant below.

The modulus values were calculated by dividing the change in applied stress, $\Delta\sigma_a$, by the corresponding change in strain, $\Delta\varepsilon$, over the interval between the succeeding points, i.e.

$$E = \frac{\Delta\sigma_a}{\Delta\varepsilon} \quad . \tag{1}$$

When calculating modulus values care should be taken to realize what affect calculations have on the resulting values. This modulus, for example, represents the stiffness of the bed when compacting the entire bed and includes the effects of wall friction. If the transmitted stress were used, the effects of wall friction would be removed, but the effective surface area of the bed is not clearly defined because of reduced stress levels acting on the regions of the bed near the wall. One might be tempted to average the two values. It is difficult to say what this would represent since the distribution of force transmitted to the wall is not known. The stress values presented here were not averaged. The choice of what modulus is used depends on the application.

The sound speed was calculated using the following propagation rate formula[2]

$$v = \sqrt{\frac{1}{\rho_s}\frac{d\sigma_s}{d\xi_s}} \quad , \tag{2}$$

where σ_s is the applied intergranular stress, ξ_i is the bed porosity, and ρ_s is the theoretical maximum density (TMD) of the propellant. The porosity is calculated from the strain, using the propellant TMD and initial bulk density, ρ_s and ρ_i respectively, using the following relationship,

$$\xi(\varepsilon) = 1 - \frac{\rho_i}{\rho_s (1-\varepsilon)} \quad . \tag{3}$$

These densities are provided in Table 2.

3.1 JA2 Response. Figures 2 and 6 show the relationships among the stress, strain, modulus, sound speed, and porosity, as indicated in the captions. The applied and transmitted stress at each temperature closely followed each other in form and magnitude at each temperature, with the transmitted stress always being lower than the applied. The stress measured at the center followed the form of the other stresses, but the magnitude varied considerably, as shown in Figure 2. This may be due to few numbers of grains in contact with the gage at the center. The JA2 grains are the largest of the three propellants tested here and in other studies were shown produce much more variation than smaller grains tested under similar conditions. At lower temperatures the value of the maximum strain was reduced due to the increased stiffness of the bed. Modulus values were very low at high temperature and much higher and more scattered at low temperature. Note that for the high temperature curve at high compression, where the porosity was below 0.1, the modulus began to increase more rapidly than the linear extension of the curve would have predicted. This was the only case in which this more rapid upswing was observed, and also the only one where the porosity had such low values. These low porosity values may be artificially low due to propellant extrusion around the edges of the ram (observed at high temperature for JA2), and errors in measurement of the initial volume of the bed, both of which critically influence the magnitude of the porosity as it approaches zero. The sound speed tracks the modulus values, as is expected from the equations. The scatter in the modulus and velocity curves at low temperature indicated that rapid relaxation of the stress occurred due to fracture or some other mechanism causing sudden fluctuation of stress.

Figure 7 shows photographs of typical damaged JA2 grains which provide evidence of the deformation mode. The grains at 52°C and 23°C deformed plastically. There was no indication of fracture or tearing. The extreme softness of the high temperature grains allowed compaction to near theoretical maximum density, and caused gross deformation as grains twisted around each other as shown in Figure 7a. After compaction the grains were pressed into a "puck" which maintained shape without support and was difficult to break apart. Plastic deformation of a much smaller degree occurred at 23°C. No gross fracture was indicated in the stress-strain curve at low temperature.

However, as mentioned above the modulus curve indicated fracture. This fracture is shown in Figure 7c where the grains appear to have chipped at stress concentration points within the bed. No plastic deformation was noted. JA2 is known to undergo a glass transition near -20°C (depending on deformation rate), which explains the change in response. The photographs show that JA2 propellant did not suffer much fracture damage in these experiments.

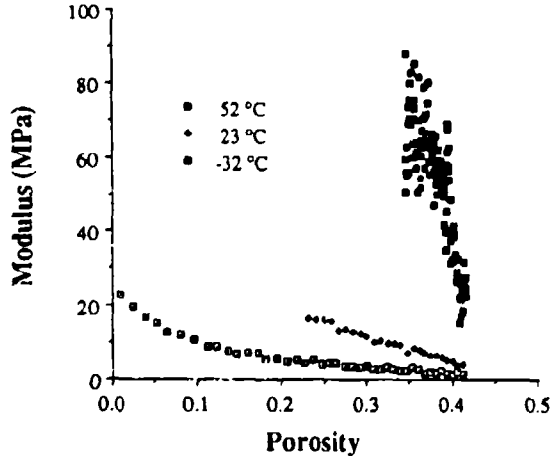

a. Bed Modulus vs Porosity

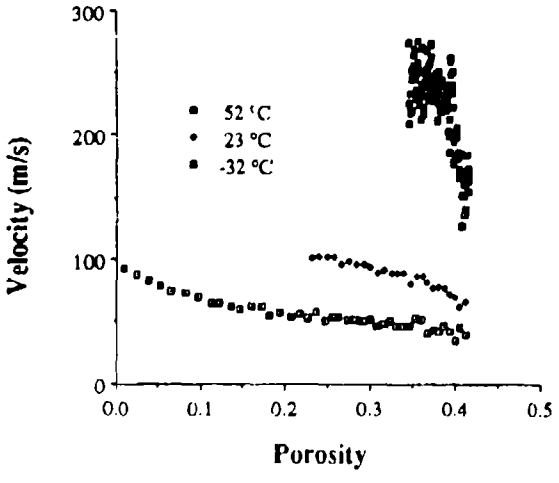

b. Sound Speed vs Porosity

Figure 6. Bed Parameters for JA2

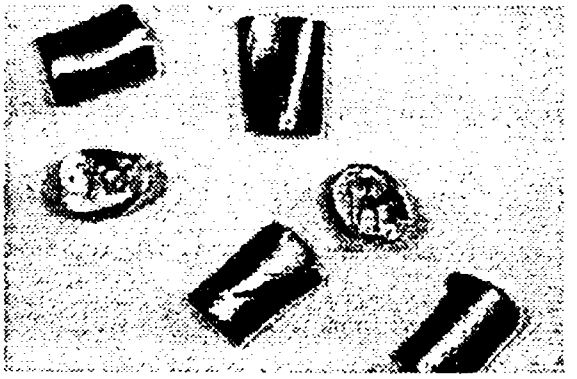

a. 52 °C

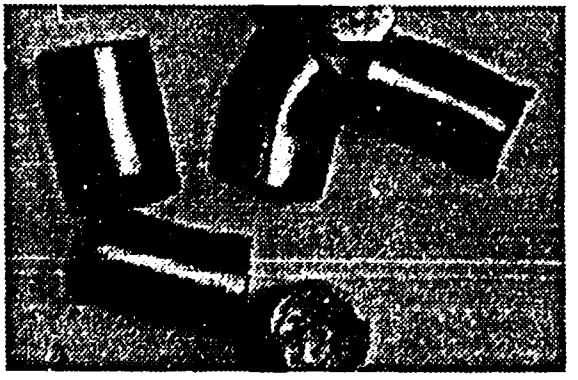

b. 23 °C

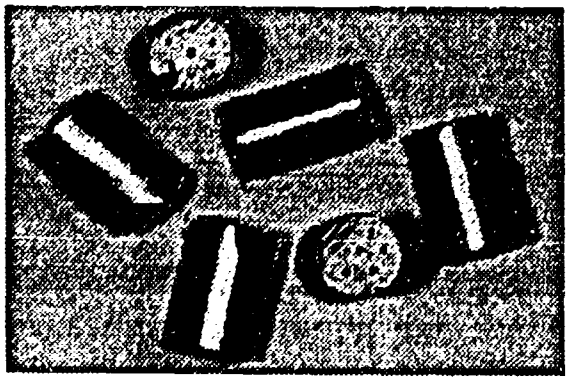

c. -32 °C

Figure 7. Photographs of Damaged JA2 Grains from the Compressed Bed

3.2 M30 Response. Figures 3 and 8 show the same relationships for M30 that were shown above for JA2. The applied and transmitted stresses followed each other in the same relationship as indicated for JA2. However, the center stress almost matched the applied stress in each case, which may be the result of the smaller grains allowing a better statistical representation on the center portion of the bed. At 52°C and 23°C the modulus and sound speed values for M30 were significantly higher than for JA2. At -32°C these values are much closer for the two propellants but the scatter was different. JA2 began compaction with little scatter which grew as the porosity decreased. The scatter in M30 began immediately upon compression, indicating an earlier onset of fracture damage.

Figure 9 shows the type of damage observed in the M30 beds. At the high temperature most deformation was plastic, although some tearing also occurred. Since the strain level was significantly less than for the JA2 propellant, less deformation was observed. At 23°C plastic deformation was observed along with chipping and crushing of grains at the stress concentration sites near the ends of the grain. Significant fracture occurred at low temperature. Most of the damaged grains were split, as shown, but chipping and crushing were also observed with little or no plastic deformation observed. This more gradual transition to fracture as the temperature was reduced, as compared to JA2, is also reflected in results of single grain deformation experiments[12]. It should be noted that, by far, most grains within the bed suffered very little or no apparent damage. The photographs show the most damaged grains. Closed bomb testing will be done to provide overall evaluation of the fracture damage of the propellant bed.

3.3 M43 Response. The same set of information provided above for JA2 and M30 propellants is presented for M43 in Figures 4 and 10. Again the center stress closely followed the applied stress at the higher temperatures, with the form of the transmitted stress curve the same as the applied, but of lesser magnitude. At low temperature stress was relieved by fracture as can be seen by the sudden drop in stress at fairly regular intervals. Note that there were corresponding drops in the center and transmitted stresses, indicating that single events were responsible for the stress reduction. The modulus and velocity curves show large scatter indicating that fracture was a major contributor to the failure process at 23°C and 52°C, as well. No modulus (or sound speed) calculations were made at -32°C. The stress vs strain curve indicated that fracture began almost immediately upon compaction giving such calculations little value.

The photographs of damaged grains are presented in Figure 11. They show what was indicated in the response curves. At the higher temperatures the grains were crushed, fractured and deformed. At low temperature splitting, chipping and the production of small chards indicated that fracture had

become the main mode of failure. Note that little plastic deformation was observed. Video tapes were made of all bed tests and the low temperature M43 test produced popping sounds (like popcorn popping) that corresponded well to the sudden reductions in magnitude found on the stress curve.

3.4 Bed and Grain Mechanical Properties. The uniaxial compressive mechanical response

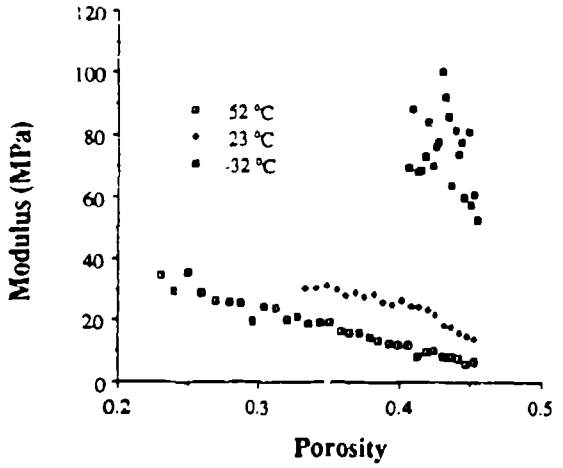

a. Bed Modulus vs Porosity

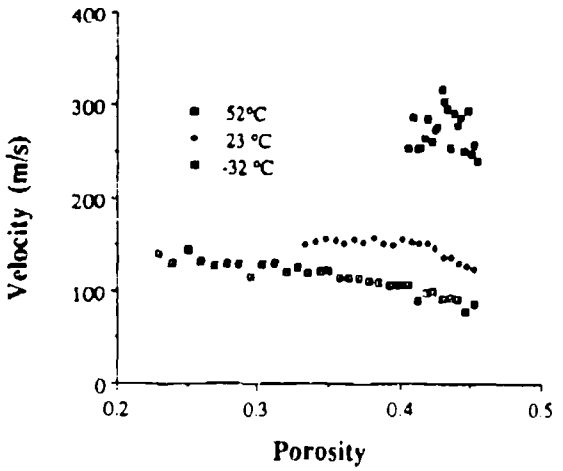

b. Sound Speed vs Porosity

Figure 8. Bed Parameters for M30

a. 52 °C

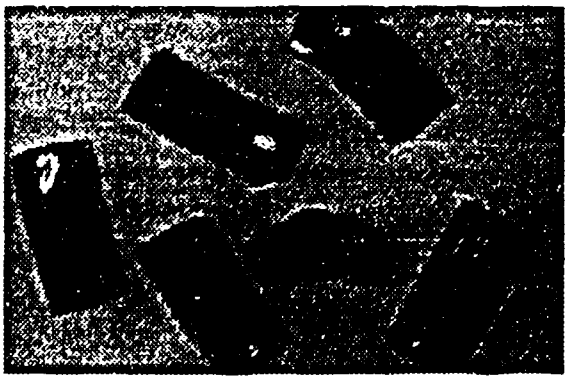

b. 23 °C

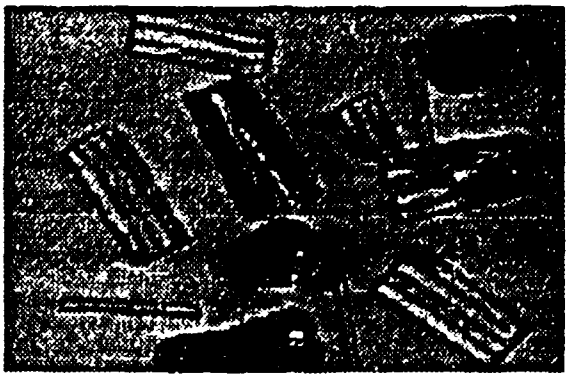

c. -32 °C

Figure 9. Photographs of Damaged M30 Grains from the Compressed Bed

of these individual propellant grains is well known. Figure 12 shows the modulus vs temperature for single grains undergoing uniaxial compression[10,11] at the same temperatures used in this study. For comparison, Figure 13 shows the modulus of the propellant beds at the higher temperatures. In previous work[8], it was shown that the grain response was reflected in the bed response, i.e. stiffer grains produced stiffer beds.

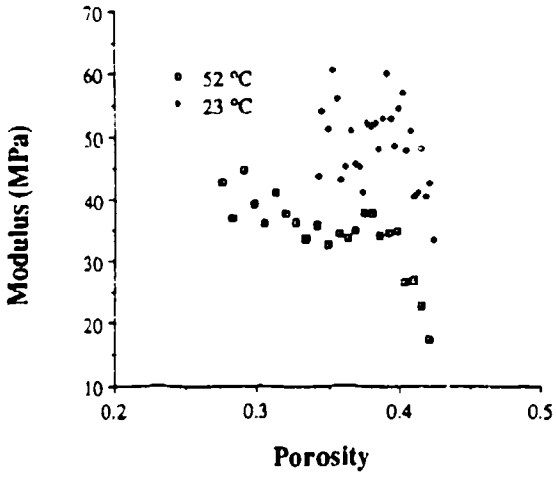

a. Bed Modulus vs Porosity

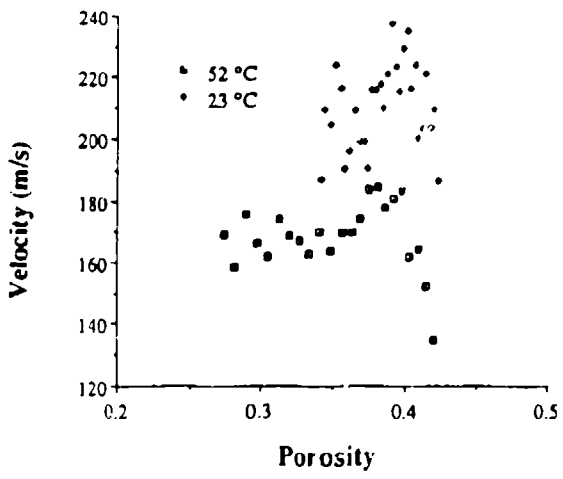

b. Sound Speed vs Porosity

Figure 10. Bed Parameters for M43

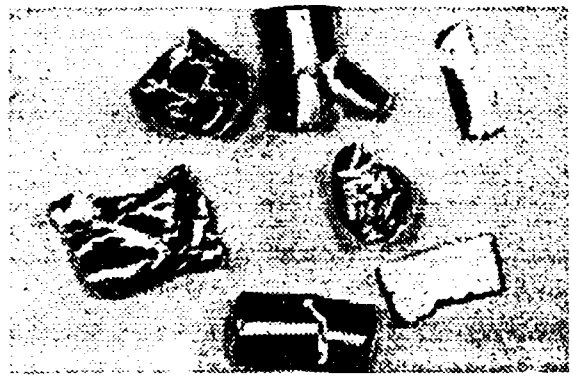

a. 52 °C

b. 23 °C

c. -32 °C

Figure 11. Photographs of Damaged M43 Grains from the Compressed Bed

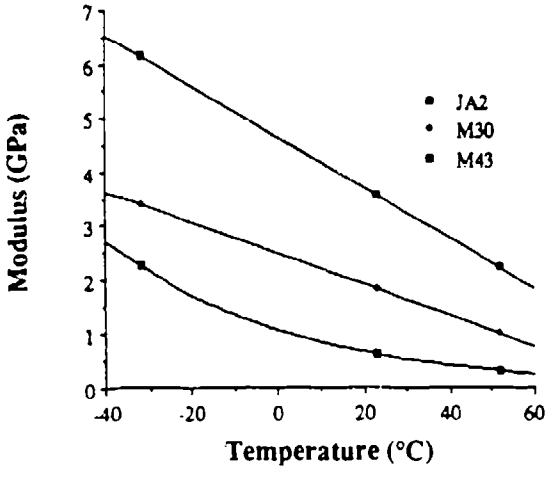

Figure 12. Modulus vs Temperature for Individual Propellant Grains at 100 s^{-1}

That same result is shown here as well. To better understand the nature of this relationship, the bed moduli were averaged over the common porosity values of the bed compaction tests (shaded area in Figure 13) and plotted against the modulus values of the individual grains. Figure 14 shows this plot and demonstrates the strong correlation of the grain and bed modulus over this porosity range, irrespective of propellant type and temperature. This result may be useful in predicting bed modulus values from individual grain response measurements.

3.5 Stress Transmitted to the Bed Wall. The measurement of the stresses transmitted to the bed wall is presented in Figure 15 for each of the propellants. A general observation is that as the applied stress increased, the stress transmitted to the wall increased in proportion. Except for JA2 at low temperature, the plots of this difference are near linear in each case indicating that the same percentage of applied stress was being supported by the wall for each curve. For M30 and M43 here is little variation of the slopes of these curves, indicating that the stress being supported by the wall was a strong function propellant surface conditions, and was not sensitive to the properties of the

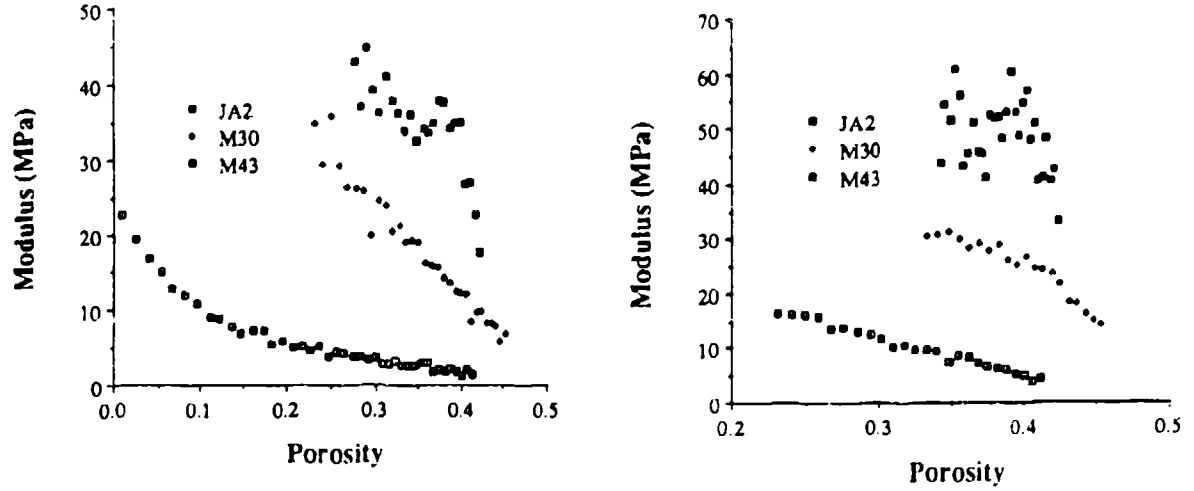

a. 52°C

b. 23°C

Figure 13. Modulus vs Porosity for JA2, M30, and M43 (Shaded Area Indicates Values Chosen for Average)

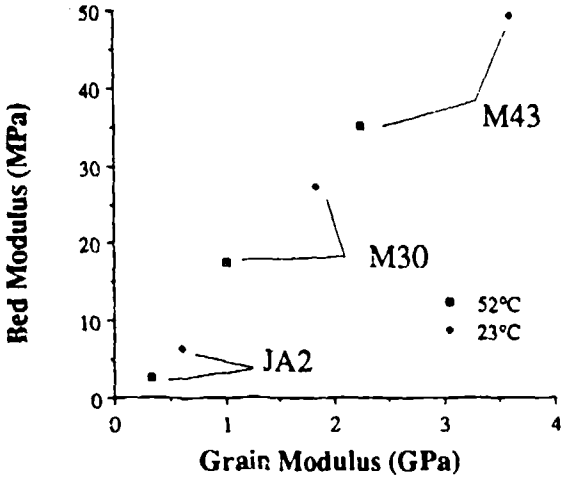

Figure 14. Bed Modulus vs Grain Modulus

grains or the propellant bed. The only curve to deviate significantly from this linear relationship was the low temperature JA2 beds. These beds experienced sticking, as indicated in Figure 2c by the nonzero applied stress with the center and transmitted stresses strating at zero. This would occur if the ram was somehow stuck to the wall at the start of the compaction. In Figure 15a note that at applied stress levels of greater than 2 MPa the curve becomes a near straight line. This could indicate the response of the bed without the early sticking. It seems that as JA2 changes dramatically from a soft, plastic response at high temperature to a hard, more brittle response at low, less of the applied force is communicated to the bed wall. At 52°C, 30 percent of the applied force was supported by the wall, at 23°C the support was reduced to 17 percent, and at -32°C, using the linear portion of the curve, the level was further reduced to about 6 percent The less dramatic change in response shown by M30 and M43 curves which were much closer together.

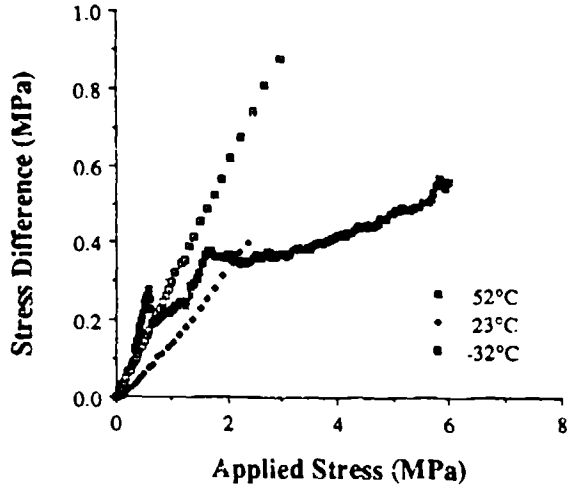

a. JA2

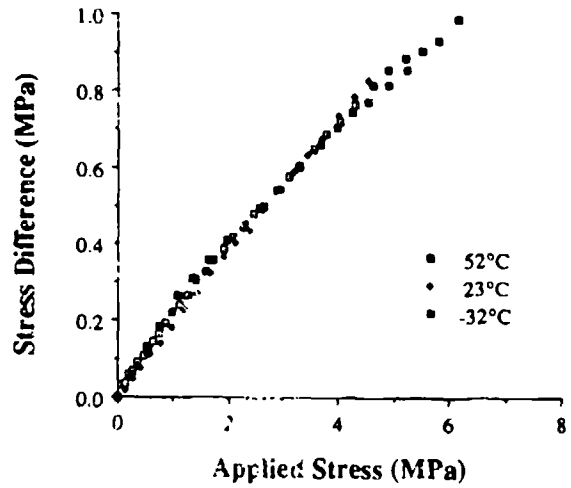

b. M30

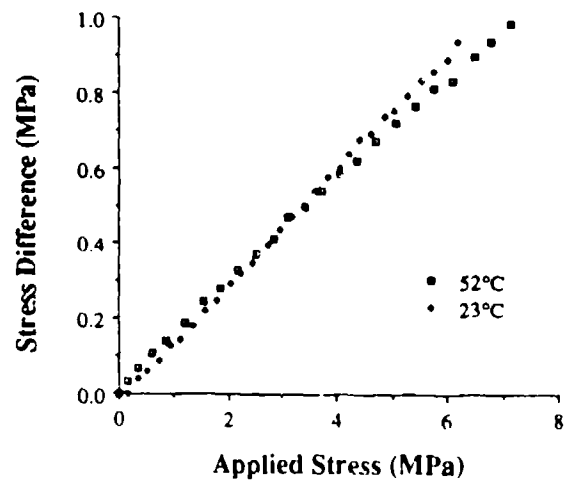

c. M43

Figure 15. Difference between the Applied and Transmitted Stress vs Applied Stress

The slopes of these curves range from 0.14 to about 0.18, indicating the portion of the applied stress supported by the bed wall.

4. CONCLUSIONS

Bed compaction tests were performed at 52°C, 23°C, and -32°C using three gun propellants, JA2, M30 and M43. These tests provided measurements of the stress applied to the bed, the stress at the center of the bed, the stress transmitted through the bed, and the strain. The mechanical response of the propellants showed significant differences. JA2 showed a soft, plastic response at higher temperatures and a stiffer low temperature response with little deformation and little fracture. M30 fractured at all temperatures with the high temperature response being softer with more tearing than brittle fracture, while at lower temperatures the stiffness and brittle response increased with a cleaving-like fracture becoming the major failure mode. M43 suffered the most damage at all temperatures. At 52°C crushing and fracture occurred, and at lower temperatures brittleness increased with increased fracture damage and smaller shards. As expected, the bed modulus increased as temperature and porosity decreased, with significant nonlinear increases observed for the modulus values at low porosity for JA2.

The velocity of mechanical disturbances was calculated from response measurements and ranged between about 50m/s for JA2 at low porosity and high temperature to over 300 m/s for M30 at low temperature. Values for propellant that underwent fracture failure, such as M43, were scattered. Meaningful velocity calculations could not be made for M43 at low temperature due to the excessive stress fluctuation recorded during compression. These values are considerably lower than historical values (440 m/s) that have been reported for other propellants[12].

The communication of applied stress to the bed wall was shown to be a linear function of the applied stress, regardless of temperature, for both M30 and M43 propellants. The level of stress supported by the wall ranged between 14 and 18 percent for these propellants . For JA2 the relationship also was linear for the higher temperatures, but the level of wall support had considerably more variation with temperature than for the other propellants, possibly due to the much greater change of the propellant response with temperature, which resulted in a greater change in the level of surface interaction between the grains and between the grains and the bed wall.

The stress values at the center of the bed followed the same form as the applied and transmitted stresses, and in most cases (except for JA2 at 52°C) the center stress also matched in magnitude. This indicates that the stress across the bed is uniform to a high degree. The earlier reports[9] of large stresses

at the center were not observed here and are now believed to have resulted from a data acquisition error.

A strong correlation was demonstrated between the bed and the single grain modulus. Other factors such as grain and bed dimensions may play a significant role. The range of grain size was small, so its role may not have been observed. This correlation offers the hope that bed properties may be able to be predicted from grain properties.

5. FUTURE STUDIES

Although these studies have shown interesting bed responses and very useful relationships between grain and bed response properties, predictions of bed stresses from ballistic codes indicate that stress levels much higher than recorded here may occur within beds during the ballistic cycle. To achieve these higher stresses a larger machine is required. It is also desired that full scale testing be done to eliminate potential problems with scaling these tests to the full sized bed. To achieve a stress of 150 MPa on a 120-mm bed a force of 1.70 MN (373,000 lb) is required. Steps are being taken to perform tests on full scale gun propellant beds using a 300 ton press at the Naval Surface Warfare Center at White Oak[6].

Intentionally Left Blank

5. REFERENCES

1. K. P. Resnik, "Charge Development for Advanced 105-mm Penetrator," 22nd JANNAF Combustion Meeting, CPIA Publication 432, Vol. II, pp 471-482, October 1985.

2. P. A. Gough, "Numerical Analysis of a Two-Phase Flow with Explicit Internal Boundaries," Final Report on Contract N00174-75-C-0259, Report # PGA-TR-76-2, Naval Ordnance Station, Indian Head, Maryland, September 1976.

3. P. Lu, B. Strauss, S. Moy, and R. Lieb. "Shaped Charge Jet Impact on Gun Propellants Study I - Temperature and Mechanical Properties Effects," 1991 Propulsion Systems Hazards Subcommittee Meeting, March 1991.

4. J. A. Birkett, "The Acquisition of M30A1 Propellant Rheology Data," Indian Head Technical Report 724, Naval Ordnance Station, Indian Head, Maryland, September 1981.

5. P. J. Coyne, and W. L. Elban, "A Strain Rate Sensitivity Prediction for Porous Bed Compaction," Proceedings of the 1983 APS Topical Conference on Shock Waves in Condensed Matter, Santa Fe, New Mexico, July 1983.

6. H. W. Sandusky, W. E. Elban, and T. P. Liddiard, "Compaction of Porous Beds," Proceedings of the 1983 APS Topical Conference on Shock Waves in Condensed Matter, Santa Fe, New Mexico, July 1983.

7. G. Zimmermann, "Investigations of Irregular Gas Pressure Rises During the Ignition of Granular Propellant of the M30 Type," Proceedings of the Eighth International Symposium on Ballistics, Orlando, Florida, October 1984.

8. R. J. Lieb, "High Strain Rate Bed Response of Gun Propellant," 1987 JANNAF Structures and Mechanical Behavior Subcommittee Meeting, CPIA Publication 463, pp51-62, March 1987.

9. R. J. Lieb, "Bed Testing of Gun Propellants at High Strain," 1991 JANNAF Structures and Mechanical Behavior Subcommittee Meeting, CPIA Publication 566, pp243-249, May 1991.

10. G.A. Gazonas, "The Mechanical Response of M30, XM39, and JA2 Propellants at Strain Rates from 10^{-2} to 250 sec^{-1}" Technical Report BRL-TR-3181, USA Laboratory Command, Ballistic Research Laboratory, Aberdeen Proving Ground, Maryland, January 1991.

11. R. J. Lieb, and M.G. Leadore, "Mechanical Failure Parameters in Gun Propellants," Technical Report BRL-TR-3296, USA Laboratory Command, Ballistic Research Laboratory, Aberdeen Proving Ground, Maryland, November 1991.

12. W. G. Soper, "Ignition Waves in Gun Chambers," Combustion and Flame, Vol. 20, pp. 157-162, 1973.

13. P. J. Conroy, "Rheological Studies Related to Interior Ballistics: A Historical Perspective," Memorandum Report BRL-MR-3970, USA Laboratory Command, Ballistic Research Laboratory, Aberdeen Proving Ground, Maryland, May 1992.

No. of
Copies Organization

2 Administrator
Defense Technical Info Center
ATTN: DTIC-DDA
Cameron Station
Alexandria, VA 22304-6145

1 Commander
U.S. Army Materiel Command
ATTN: AMCAM
5001 Eisenhower Ave.
Alexandria, VA 22333-0001

1 Director
U.S. Army Research Laboratory
ATTN: AMSRL-D
2800 Powder Mill Rd.
Adelphi, MD 20783-1145

1 Director
U.S. Army Research Laboratory
ATTN: AMSRL-OP-CI-AD,
Tech Publishing
2800 Powder Mill Rd.
Adelphi, MD 20783-1145

2 Commander
U.S. Army Armament Research,
Development, and Engineering Center
ATTN: SMCAR-IMI-I
Picatinny Arsenal, NJ 07806-5000

2 Commander
U.S. Army Armament Research,
Development, and Engineering Center
ATTN: SMCAR-TDC
Picatinny Arsenal, NJ 07806-5000

1 Director
Benet Weapons Laboratory
U.S. Army Armament Research,
Development, and Engineering Center
ATTN: SMCAR-CCB-TL
Watervliet, NY 12189-4050

(Unclass. only)1 Commander
U.S. Army Rock Island Arsenal
ATTN: SMCRI-IMC-RT/Technical Library
Rock Island, IL 61299-5000

1 Director
U.S. Army Aviation Research
and Technology Activity
ATTN: SAVRT-R (Library)
M/S 219-3
Ames Research Center
Moffett Field, CA 94035-1000

No. of
Copies Organization

1 Commander
U.S. Army Missile Command
ATTN: AMSMI-RD-CS-R (DOC)
Redstone Arsenal, AL 35898-5010

1 Commander
U.S. Army Tank-Automotive Command
ATTN: ASQNC-TAC-DIT (Technical
Information Center)
Warren, MI 48397-5000

1 Director
U.S. Army TRADOC Analysis Command
ATTN: ATRC-WSR
White Sands Missile Range, NM 88002-5502

1 Commandant
U.S. Army Field Artillery School
ATTN: ATSF-CSI
Ft. Sill, OK 73503-5000

(Class. only)1 Commandant
U.S. Army Infantry School
ATTN: ATSH-CD (Security Mgr.)
Fort Benning, GA 31905-5660

(Unclass. only)1 Commandant
U.S. Army Infantry School
ATTN: ATSH-CD-CSO-OR
Fort Benning, GA 31905-5660

1 WL/MNOI
Eglin AFB, FL 32542-5000

Aberdeen Proving Ground

2 Dir, USAMSAA
ATTN: AMXSY-D
AMXSY-MP, H. Cohen

1 Cdr, USATECOM
ATTN: AMSTE-TC

1 Dir, ERDEC
ATTN: SCBRD-RT

1 Cdr, CBDA
ATTN: AMSCB-CI

1 Dir, USARL
ATTN: AMSRL-SL-I

10 Dir, USARL
ATTN: AMSRL-OP-CI-B (Tech Lib)

No. of
Copies Organization

1 Chairman
DOD Explosives Safety Board
Room 856-C
Hoffman Bldg. 1
2461 Eisenhower Avenue
Alexandria, VA 22331-0600

1 Headquarters
U.S. Army Materiel Command
ATTN: AMCICP-AD, M. Fisette
5001 Eisenhower Ave.
Alexandria, VA 22333-0001

1 U.S. Army Ballistic Missile
Defense Systems Command
Advanced Technology Center
P.O. Box 1500
Huntsville, AL 35807-3801

1 Department of the Army
Office of the Product Manager
155mm Howitzer, M109A6,
Paladin
ATTN: SFAE-AR-HIP-IP,
Mr. R. De Kleine
Picatinny Arsenal, NJ 07806-5000

3 Project Manager
Advanced Field Artillery System
ATTN: SFAE-ASM-AF-E
LTC D. Ellis
T. Kuriata
J. Shields
Picatinny Arsenal, NJ 07801-5000

1 Project Manager
Advanced Field Artillery System
ATTN: SFAE-ASM-AF-Q, W. Warren
Picatinny Arsenal, NJ 07801-5000

2 Commander
Production Base Modernization
Agency
U.S. Army Armament Research,
Development, and
Engineering Center
ATTN: AMSMC-PBM, A. Siklosi
AMSMC-PBM-E, L. Laibson
Picatinny Arsenal, NJ 07806-5000

No. of
Copies Organization

4 PEO-Armaments
Project Manager
Tank Main Armament System
ATTN: AMCPM TMA
AMCPM-TMA-105
AMCPM-TMA-120
AMCPM-TMA-AS, H. Yuen
Picatinny Arsenal, NJ 07806-5000

5 Commander
U.S. Army Armament Research,
Development, and
Engineering Center
ATTN: SMCAR-CCD, D. Spring
SMCAR-CCH-V, C. Mandala
E. Fennell
SMCAR-CCH-T, L. Rosendorf
SMCAR-CCS
Picatinny Arsenal, NJ 07806-5000

19 Commander
U.S. Army Armament Research,
Development, and Engineering
Center
ATTN: SMCAR-AEE, J. Lannon
SMCAR-AEE-B,
A. Beardell
D. Downs
S. Einstein
S. Westley
S. Bernstein
J. Rutkowski
B. Brodman
P. O'Reilly
R. Cirincione
A. Grabowsky
P. Hui
J. O'Reilly
SMCAR-AEE-WW,
M. Mezger
J. Pinto
D. Wiegand
P. Lu
C. Hu
SMCAR-AES, S. Kaplowitz
Picatinny Arsenal, NJ 07806-5000

1 Commander
U.S. Army Armament Research,
Development and Engineering
Center
ATTN: SMCAR-HFM, E. Barrieres
Picatinny Arsenal, NJ 07806-5000

No. of Copies	Organization
9	Commander U.S. Army Armament Research, Development and Engineering Center ATTN: SMCAR-FSA-T, M. Salsbury SMCAR-FSA-F, LTC R. Riddle SMCAR-FSC, G. Ferdinand SMCAR-FS, T. Gora SMCAR-FS-DH, J. Feneck SMCAR-FSS-A, R. Kopman B. Machek L. Pinder SMCAR-FSN-N, K. Chung Picatinny Arsenal, NJ 07806-5000
3	Director Benet Weapons Laboratories ATTN: SMCAR-CCB-RA, G.P. O'Hara G.A. Pflegl SMCAR-CCB-S, F. Heiser Watervliet, NY 12189-4050
2	Commander U.S. Army Research Office ATTN: Technical Library D. Mann P.O. Box 12211 Research Triangle Park, NC 27709-2211
1	Commander, USACECOM R&D Technical Library ATTN: ASQNC-ELC-IS-L-R, Myer Center Fort Monmouth, NJ 07703-5301
1	Commander U.S. Army Harry Diamond Laboratory ATTN: SLCHD-TA-L 2800 Powder Mill Rd. Adelphi, MD 20783-1145
1	Commandant U.S. Army Aviation School ATTN: Aviation Agency Fort Rucker, AL 36360
1	Program Manager U.S. Tank-Automotive Command ATTN: AMCPM-ABMS, T. Dean Warren, MI 48092-2498

No. of Copies	Organization
1	Project Manager U.S. Tank-Automotive Command Fighting Vehicle Systems ATTN: SFAE-ASM-BV Warren, MI 48397-5000
1	Project Manager, Abrams Tank System ATTN: SFAE-ASM-AB Warren, MI 48397-5000
1	Director HQ, TRAC RPD ATTN: ATCD-MA Fort Monroe, VA 23651-5143
2	Director U.S. Army Materials Technology Laboratory ATTN: SLCMT-ATL (2 cps) Watertown, MA 02172-0001
1	Commander U.S. Army Belvoir Research and Development Center ATTN: STRBE-WC Fort Belvoir, VA 22060-5006
1	Director U.S. Army TRAC-Ft. Lee ATTN: ATRC-L, Mr. Cameron Fort Lee, VA 23801-6140
1	Commandant U.S. Army Command and General Staff College Fort Leavenworth, KS 66027
1	Commandant U.S. Army Special Warfare School ATTN: Rev and Trng Lit Div Fort Bragg, NC 28307
1	Commander Radford Army Ammunition Plant ATTN: SMCAR-QA/HI LIB Radford, VA 24141-0298

No. of
Copies Organization

1 Commander
U.S. Army Foreign Science and
Technology Center
ATTN: AMXST-MC-3
220 Seventh Street, NE
Charlottesville, VA 22901-5396

2 Commandant
U.S. Army Field Artillery
Center and School
ATTN: ATSF-CO-MW, E. Dublisky
ATSF-CN, P. Gross
Ft. Sill, OK 73503-5600

1 Commandant
U.S. Army Armor School
ATTN: ATZK-CD-MS, M. Falkovitch
Armor Agency
Fort Knox, KY 40121-5215

2 Commander
Naval Sea Systems Command
ATTN: SEA 62R
SEA 64
Washington, DC 20362-5101

1 Commander
Naval Air Systems Command
ATTN: AIR-954-Tech Library
Washington, DC 20360

4 Commander
Naval Research Laboratory
ATTN: Technical Library
Code 4410, K. Kailasanate
J. Boris
E. Oran
Washington, DC 20375-5000

1 Office of Naval Research
ATTN: Code 473, R.S. Miller
800 N. Quincy Street
Arlington, VA 22217-9999

1 Office of Naval Technology
ATTN: ONT-213, D. Siegel
800 N. Quincy St.
Arlington, VA 22217-5000

No. of
Copies Organization

4 Commander
Naval Surface Warfare Center
ATTN: Code 730
Code R-13,
R. Bernecker
H. Sandusky
Silver Spring, MD 20903-5000

7 Commander
Naval Surface Warfare Center
ATTN: T.C. Smith
K. Rice
S. Mitchell
S. Peters
J. Consaga
C. Gotzmer
Technical Library
Indian Head, MD 20640-5000

5 Commander
Naval Surface Warfare Center
ATTN: Code G30,
Code G32,
Code G33, J.L. East
T. Doran
Code E23 Technical Library
Dahlgren, VA 22448-5000

5 Commander
Naval Air Warfare Center
ATTN: Code 388, C.F. Price
T. Boggs
Code 3895, T. Parr
R. Derr
Information Science Division
China Lake, CA 93555-6001

2 Commanding Officer
Naval Underwater Systems Center
ATTN: Code 5B331, R.S. Lazar
Technical Library
Newport, RI 02840

1 AFOSR/NA
ATTN: J. Tishkoff
Bolling AFB, D.C. 20332-6448

1 OLAC PL/TSTL
ATTN: D. Shiplett
Edwards AFB, CA 93523-5000

No. of
Copies Organization

3 AL/LSCF
ATTN: J. Levine
L. Quinn
T. Edwards
Edwards AFB, CA 93523-5000

1 WL/MNAA
ATTN: B. Simpson
Eglin AFB, FL 32542-5434

1 WL/MNME
Energetic Materials Branch
2306 Perimeter Rd.
STE 9
Eglin AFB, FL 32542-5910

1 WL/MNSH
ATTN: R. Drabczuk
Eglin AFB, FL 32542-5434

2 NASA Langley Research Center
ATTN: M.S. 408, W. Scallion
D. Witcofski
Hampton, VA 23605

1 Central Intelligence Agency
Office of the Central References
Dissemination Branch
Room GE-47, HQS
Washington, DC 20502

1 Central Intelligence Agency
ATTN: J. Backofen
HQ Room 5FL2
Washington, DC 20505

1 SDIO/TNI
ATTN: L.H. Caveny
Pentagon
Washington, DC 20301-7100

1 SDIO/DA
ATTN: E. Gerry
Pentagon
Washington, DC 21301-7100

2 HQ DNA
ATTN: D. Lewis
A. Fahey
6801 Telegraph Rd.
Alexandria, VA 22310-3398

No. of
Copies Organization

1 Director
Sandia National Laboratories
Energetic Materials & Fluid Mechanics
Department, 1512
ATTN: M. Baer
P.O. Box 5800
Albuquerque, NM 87185

1 Director
Sandia National Laboratories
Combustion Research Facility
ATTN: R. Carling
Livermore, CA 94551-0469

4 Director
Lawrence Livermore National
Laboratory
ATTN: L-355,
A. Buckingham
G. Benedetti
M. Finger
L-324, M. Constantino
P.O. Box 808
Livermore, CA 94550-0622

2 Director
Los Alamos Scientific Lab
ATTN: T3/D. Butler
M. Division/B. Craig
P.O. Box 1663
Los Alamos, NM 87544

3 Battelle Columbus Laboratories
ATTN: TACTEC Library,
J.N. Huggins
V. Levin
505 King Avenue
Columbus, OH 43201-2693

1 Battelle PNL
ATTN: Mr. Mark Garnich
P.O. Box 999
Richland, WA 99352

1 Institute of Gas Technology
ATTN: D. Gidaspow
3424 S. State Street
Chicago, IL 60616-3896

No. of Copies Organization

1 Institute for Advanced Technology
ATTN: T.M. Krehne
The University of Texas of Austin
4030-2 W. Braker Lane
Austin, TX 78759-5329

2 CPIA - JHU
ATTN: Hary J. Hoffman
T. Christian
10630 Little Patuxent Parkway
Suite 202
Columbia, MD 21044-3200

1 Brigham Young University
Department of Chemical Engineering
ATTN: M. Beckstead
Provo, UT 84601

1 Jet Propulsion Laboratory
California Institute of Technology
ATTN: L.D. Strand, MS 125/224
4800 Oak Grove Drive
Pasadena, CA 91109

1 California Institute of Technology
204 Karman Lab
Main Stop 301-46
ATTN: F.E.C. Culick
1201 E. California Street
Pasadena, CA 91109

3 Georgia Institute of Technology
School of Aerospace Engineering
ATTN: B.T. Zim
E. Price
W.C. Strahle
Atlanta, GA 30332

1 Massachusetts Institute of Technology
Department of Mechanical Engineering
ATTN: T. Toong
77 Massachusetts Avenue
Cambridge, MA 02139-4307

1 University of Illinois
Department of Mechanical/Industry
Engineering
ATTN: H. Krier
144 MEB; 1206 N. Green St.
Urbana, IL 61801-2978

No. of Copies Organization

1 University of Maryland
ATTN: Dr. J.D. Anderson
College Park, MD 20740

1 University of Massachusetts
Department of Mechanical Engineering
ATTN: K. Jakus
Amherst, MA 01002-0014

1 University of Minnesota
Department of Mechanical Engineering
ATTN: E. Fletcher
Minneapolis, MN 55414-3368

3 Pennsylvania State University
Department of Mechanical Engineering
ATTN: V. Yang
K. Kuo
C. Merkle
University Park, PA 16802-7501

1 Rensselaer Polytechnic Institute
Department of Mathematics
Troy, NY 12181

1 Stevens Institute of Technology
Davidson Laboratory
ATTN: R. McAlevy III
Castle Point Station
Hoboken, NJ 07030-5907

1 Rutgers University
Department of Mechanical and
Aerospace Engineering
ATTN: S. Temkin
University Heights Campus
New Brunswick, NJ 08903

1 University of Southern California
Mechanical Engineering Department
ATTN: OHE200, M. Gerstein
Los Angeles, CA 90089-5199

1 University of Utah
Department of Chemical Engineering
ATTN: A. Baer
Salt Lake City, UT 84112-1194

1 Washington State University
Department of Mechanical Engineering
ATTN: C.T. Crowe
Pullman, WA 99163-5201

No. of Copies	Organization
1	AFELM, The Rand Corporation ATTN: Library D 1700 Main Street Santa Monica, CA 90401-3297
1	Arrow Technology Associates, Inc. ATTN: W. Hathaway P.O. Box 4218 South Burlington, VT 05401-0042
3	AAI Corporation ATTN: J. Hebert J. Frankle D. Cleveland P.O. Box 126 Hunt Valley, MD 21030-0126
2	Alliant Techsystems, Inc. ATTN: R.E. Tompkins J. Kennedy 7225 Northland Dr. Brooklyn Park, MN 55428
1	AVCO Everett Research Laboratory ATTN: D. Stickler 2385 Revere Beach Parkway Everett, MA 02149-5936
1	General Applied Sciences Lab ATTN: J. Erdos 77 Raynor Ave. Ronkonkama, NY 11779-6649
1	General Electric Company Tactical System Department ATTN: J. Mandzy 100 Plastics Ave. Pittsfield, MA 01201-3698
1	IITRI ATTN: M.J. Klein 10 W. 35th Street Chicago, IL 60616-3799
5	Hercules, Inc. Radford Army Ammunition Plant ATTN: D.A. Worrell W.J. Worrell R Gott C. Chandler L. Rivenbark Radford, VA 24141-0299
2	Hercules, Inc. Allegheny Ballistics Laboratory ATTN: William B. Walkup Thomas F. Farabaugh P.O. Box 210 Rocket Center, WV 26726
1	Hercules, Inc. Hercules Plaza ATTN: B.M. Riggleman Wilmington, DE 19894
1	MBR Research Inc. ATTN: Dr. Moshe Ben-Reuven 601 Ewing St., Suite C-22 Princeton, NJ 08540
1	Olin Corporation Badger Army Ammunition Plant ATTN: F.E. Wolf Baraboo, WI 53913
3	Olin Ordnance ATTN: E.J. Kirschke A.F. Gonzalez D.W. Worthington P.O. Box 222 St. Marks, FL 32355-0222
1	Olin Ordnance ATTN: H.A. McElroy 10101 9th Street, North St. Petersburg, FL 33716
1	Paul Gough Associates, Inc. ATTN: P.S. Gough 1048 South St. Portsmouth, NH 03801-5423
1	Physics International Library ATTN: H. Wayne Wampler P.O Box 5010 San Leandro, CA 94577-0599
2	Princeton Combustion Research Laboratories, Inc. ATTN: N. Mer N.A. Messina Princeton Corporate Plaza 11 Deerpark Dr., Bldg IV, Suite 119 Monmouth Junction, NJ 08852

No. of
Copies Organization

3 Rockwell International
Rocketdyne Division
ATTN: BA08,
J. Flanagan
J. Gray
R.B. Edelman
6633 Canoga Avenue
Canoga Park, CA 91303-2703

2 Rockwell International Science Center
ATTN: Dr. S. Chakravarthy
Dr. S. Palaniswamy
1049 Camino Dos Rios
P.O. Box 1085
Thousand Oaks, CA 91360

1 Southwest Research Institute
ATTN: J.P. Riegel
6220 Culebra Road
P.O. Drawer 28510
San Antonio, TX 78228-0510

1 Sverdrup Technology, Inc.
ATTN: Dr. John Deur
2001 Aerospace Parkway
Brook Park, OH 44142

2 Thiokol Corporation
Elkton Division
ATTN: R. Biddle
Tech Library
P.O. Box 241
Elkton, MD 21921-0241

1 Veritay Technology, Inc.
ATTN: E. Fisher
4845 Millersport Hwy.
East Amherst, NY 14501-0305

1 Universal Propulsion Company
ATTN: H.J. McSpadden
25401 North Central Ave.
Phoenix, AZ 85027-7837

1 SRI International
Propulsion Sciences Division
ATTN: Tech Library
333 Ravenwood Avenue
Menlo Park, CA 94025-3493

No. of
Copies Organization

Aberdeen Proving Ground

1 Cdr, USACSTA
ATTN: STECS-PO/R. Hendricksen

No. of Copies	Organization
1	Ernst-Mach-Institut ATTN: Dr. R. Heiser Haupstrasse 18 Weil am Rheim Germany
1	Defence Research Agency, Military Division ATTN: C. Woodley RARDE Fort Halstead Sevenoaks, Kent, TN14 7BP England
1	School of Mechanical, Materials, and Civil Engineering ATTN: Dr. Bryan Lawton Royal Military College of Science Shrivenham, Swindon, Wiltshire, SN6 8LA England
2	Institut Saint Louis ATTN: Dr. Marc Giraud Dr. Gunther Sheets Postfach 1260 7858 Weail am Rhein 1 Germany
1	Explosive Ordnance Division ATTN: A. Wildegger-Gaissmaier Defence Science and Technology Organisation P.O. Box 1750 Salisbury, South Australia 5108
1	Armaments Division ATTN: Dr. J. Lavigne Defence Research Establishment Valcartier 2459, Pie XI Blvd., North P.O. Box 8800 Courcelette, Quebec G0A 1R0 Canada
1	U.S. Army European Research Office ATTN: Dr. Roy E. Richenbach Box 65 FPO New York 09510-1500

INTENTIONALLY LEFT BLANK.

USER EVALUATION SHEET/CHANGE OF ADDRESS

This Laboratory undertakes a continuing effort to improve the quality of the reports it publishes. Your comments/answers to the items/questions below will aid us in our efforts.

1. ARL Report Number ARL-TR-78 Date of Report February 1993

2. Date Report Received _____

3. Does this report satisfy a need? (Comment on purpose, related project, or other area of interest for which the report will be used.) _____

4. Specifically, how is the report being used? (Information source, design data, procedure, source of ideas, etc.) _____

5. Has the information in this report led to any quantitative savings as far as man-hours or dollars saved, operating costs avoided, or efficiencies achieved, etc? If so, please elaborate. _____

6. General Comments. What do you think should be changed to improve future reports? (Indicate changes to organization, technical content, format, etc.) _____

CURRENT ADDRESS

_____
Organization

_____
Name

_____
Street or P.O. Box No.

_____
City, State, Zip Code

7. If indicating a Change of Address or Address Correction, please provide the Current or Correct address above and the Old or Incorrect address below.

OLD ADDRESS

_____
Organization

_____
Name

_____
Street or P.O. Box No.

_____
City, State, Zip Code

(Remove this sheet, fold as indicated, staple or tape closed, and mail.)